

Application of Copper Mining Waste in Radionuclide and Heavy Metal Immobilization

Slavko Dimović, Ivana Jelić,* Marija Šljivić-Ivanović, Zoran Štirbanović, Vojka Gardić, Radmila Marković, Aleksandar Savić, and Dimitrije Zakic

Copper slag flotation tailings (CSFT), as the end waste from copper mining, are evaluated for radionuclide and heavy metal immobilization. Characterization of CSFT based on grain size and mineral composition, surface functional groups, pH and electrical conductivity in aqueous media, thermogravimetric analysis (TGA), determination of characteristic temperatures in sample melting process, leachability, and toxicity tests is conducted. The screening sorption of Mn(II), Co(II), Ni(II), Zn(II), Cd(II), and Pb(II) inactive isotopes from single-component solutions is performed. The Cd(II) ions show better sorption potential than other ions, with a sorption capacity of 0.08 mmol g⁻¹ at the highest initial concentration. Sorption decreases in the sequence Cd(II) > Pb(II) > Zn(II) > Mn(II) > Ni(II) > Co(II) at all initial concentrations. Although CSFT shows lower sorption capability than synthetic sorbents based on fayalite and magnetite, its inexpensiveness and substantial accessible amount represent great advantages in wider utilization.

1. Introduction

Copper slag flotation tailings (CSFT) represent mining waste generated in the process of copper slag flotation. Copper slag is a by-product of pyrometallurgical processing of copper concentrates obtained from copper ores, containing large amounts of valuable metals. In order to recover metals from slag, the most commonly used technology is flotation.^[1–3] The average total amount of CSFT adds up to tens of millions of tons per each

copper processing facility.^[4] According to literature data, the copper production in 2016 only from primary sources, i.e., copper ores, was approximately 20 million tons and was almost doubled in the early 2000s.^[5] Since 2.2 tons of copper slag are produced for one ton of pure copper,^[6] vast quantities of this waste are generated every year. The reuse of copper slag is increased worldwide, and a considerable amount of CSFT is disposed of. Generated and accumulated CSFT represents a possible environmental threat, potentially polluting water-courses by atmospheric precipitation, wind erosion, or accidents,^[7–8] e.g., dam rupture and spilling pollutants into underground water systems.^[9]

Although CSFT represents the end waste, with a matrix composed of iron silicates, it could be utilized as a raw

material in construction industry and metallurgy, providing environmental and economic benefits. Extracting iron is the most common method for managing CSFT.^[1] Since it possesses pozzolanic properties, CSFT is used in cement and concrete production.^[10] Besides these applications, waste materials can be potentially used as environmental-friendly and low-cost sorbent materials for aqueous media purification. Thus, the various sorbents developed from different cost-effective waste sources were successfully tested, e.g., industrial sludge, ash, slag, red mud, animal bones, and construction and demolition waste.^[11–24] However, there is scarce literature data on heavy metal and radionuclide sorption onto CSFT despite great interest in new, sustainable, and effective liquid waste purification development.

Liquid radioactive waste (LRW) is produced by industries such as mining, nuclear power generation, and defense, as well as in nuclear medicine and scientific research.^[25] Chemical composition varies among LRW of different origins. For example, a real effluent contaminated with uranium during uranium mining might contain other radionuclides and stable isotopes (chromium, manganese, iron, cobalt, nickel, copper, zinc, cadmium, lead, etc.), as well as essential metals.^[26] Among radionuclides within nuclear power plants, the main activation products are ⁵⁴Mn, ^{59,63}Ni, ⁶⁰Co, and ⁶⁵Zn, produced in the reactions between nuclear reaction materials (e.g., stainless steel or Ni alloys) and radiation. As short-living isotopes, ⁵⁴Mn ($t_{1/2} = 312$ days) and ⁶⁵Zn ($t_{1/2} = 244$ days) are significant during the first year after the nuclear reactor shut down. ²¹⁰Pb can be produced by natural uranium decay, while ⁵⁹Ni and ⁶⁰Co are the most important for

S. Dimović, I. Jelić, M. Šljivić-Ivanović
 Vinca Institute of Nuclear Sciences
 University of Belgrade
 Mike Petrovića Alasa 12-14, Belgrade 11351, Serbia
 E-mail: ivana.jelic@vin.bg.ac.rs
 Z. Štirbanović
 Technical Faculty in Bor
 University of Belgrade
 Vojske Jugoslavije 12, Bor 19210, Serbia
 V. Gardić, R. Marković
 Mining and Metallurgy Institute
 Zeleni bulevar 35, Bor 19210, Serbia
 A. Savić, D. Zakic
 Faculty of Civil Engineering
 University of Belgrade
 Bulevar kralja Aleksandra 73, Belgrade 11000, Serbia

 The ORCID identification number(s) for the author(s) of this article can be found under <https://doi.org/10.1002/cfen.202000419>

DOI: 10.1002/cfen.202000419

disposal due to the long half-life of ^{59}Ni ($t_{1/2} = 76\,000$ years) and high-intensity gamma emission of ^{60}Co ($t_{1/2} = 5.3$ years). Furthermore, short-living ^{109}Cd ($t_{1/2} = 466$ days) and ^{113}Cd ($t_{1/2} = 7.7 \times 10^{15}$ years) are fission products and could also be found in nuclear reactors.^[27] Except for unstable isotopes, Mn, Co, Ni, Zn, Cd, and Pb might exist in the stable form known as toxic heavy metals. These elements are often ingredients of industrial wastewater.

The aim of this research was a brief screening of radionuclides and heavy metals immobilization by CSFT. The investigation basis was CSFT sorption capacities estimation. The satisfying sorption potential of CSFT could be expected based on favorable amounts of minerals such as magnetite and fayalite.^[28–30] For sorption experiments, the Mn(II), Co(II), Ni(II), Zn(II), Cd(II), and Pb(II) ions in single-component solutions were selected. The study also included a detailed waste characterization in order to verify CSFT effective and safe usage.

2. Materials and Methods

2.1. CSFT Characterization

The investigated CSFT originates from the old flotation tailing dump in Bor. The sample weighing approximately 2 kg was spread over 1 m² area, and 50 g were sampled from five randomly chosen points, rinsed with deionized water, and dried at 100 °C.

CSFT samples were characterized by grain size, mineral composition, surface functional groups, pH, and electrical conductivity (EC) in aqueous media. In addition, thermogravimetric analysis (TGA) and determination of characteristic temperatures in the sample melting process were explored.

Grain size composition was determined by a combination of sieving (for larger particle fractions) and hydrometer-method (for those <63 μm) according to ISO 17892-4:2016.^[31] The hydrometer method represents a standardized procedure used for grain size distribution determination, usually for particles <63 μm. Distilled water was used as a suspending fluid. In order to prevent coagulation of particles, dispersing agent was added. The results were shown by the mass and cumulative participation of the particles in the CSFT sample grain size class. The uncertainty for grain size distribution determination by sieving and hydrometer analyses is considered to be ±5%.

The mineral composition was identified by X-ray diffraction analysis (XRD) using Ultima IV Rigaku diffractometer, equipped with Cu Kα_{1,2} radiation (generator voltage (40.0 kV) and a generator current (40.0 mA)). The range of 2θ 4°–65° was used for analysis in continuous scan mode with a scanning step size of 0.02°, at a rate of 5° min⁻¹. The obtained XRD patterns were compared with the International Centre for Diffraction Data (ICDD) database.^[32]

The major functional groups at the surface of the material were identified by Fourier transform infrared (FT-IR) spectroscopy. The spectra were recorded at ambient conditions in the mid-IR region (400–4000 cm⁻¹) using a Nicolet IS 50 FT-IR spectrometer operating in the ATR mode in the resolution of 4 cm⁻¹ with 32 scans.

The pH values of CSFT were determined for different mass ratios (solid/liquid) of the samples in deionized water: 1:1, 1:10, 1:20, 1:100, and 1:200 by a modified US EPA 9045D method for determination of soil and waste pH.^[33] Suspensions were shaken

at 120 rpm for 5 min, centrifuged (at 6000 rpm for 20 min), and filtered. The measurements of pH values were conducted in both, the suspensions and the filtrates by WTW InoLab pH meter. Filtrate EC was measured simultaneously by WTW InoLab Cond 7110. The pH and EC determination tests were done in triplicate.

TGA of the CSFT sample was conducted in a corundum dish at atmospheric pressure in the air stream in a range from ambient temperature up to 1500 °C, at a temperature regime of 10 °C min⁻¹ by Leco Thermogravimetric Analyzer TGA 701. The characteristic temperatures in the sample melting process were determined in the Carbolite Fusibility Furnace CAFDIG CO/CO₂+Air.

2.2. Leachability and Toxicity of CSFT

The impact of CSFT on the environment was carried out by the leaching test, i.e., leaching procedure (LP) according to standard SRPS EN 12457-2^[34] for waste characterization by compliance test for leaching of granular waste materials and sludge. Standard prescribes a one-stage batch test at a liquid/solid (L/S) ratio of 10 L kg⁻¹ (10:1) for materials with a high content of solids and particle size of <4 mm (with or without decreasing particle size).^[34] The investigated CSFT sample that initially had at least a 95% mass ratio of particles <4 mm was brought into contact with the leachant (deionized water) under defined conditions: continuous stirring on an orbital shaking table at 10 rpm at room temperature (22 ± 2 °C), contact time of 24 h, without any pH setups. The used method presumes that the equilibrium or near-equilibrium state might be achieved between the liquid and solid phases during the test period. The ambient temperature was 21 °C, humidity of 52%, and an atmospheric pressure of 970 hPa. The eluate was separated from the solid by filtering, and its pH and EC values were measured (WTW InoLab pH-meter and WTW InoLab Cond 7110) and compared with the upper limits prescribed in the Annex 7 of the Regulation on categories, testing, and classification of waste.^[35]

The toxicity characteristic of CSFT was carried out by the toxicity characteristic leaching procedure (TCLP) according to standard US EPA 1311.^[36] The solid phase was extracted with an amount of extraction fluid (glacial acetic acid, Merck, p.a.) equal to 20 times of the solid phase weight, under defined conditions: continuous stirring on an orbital shaking table at 30 rpm at room temperature (22 ± 2 °C), with contact time of 18 h. The extraction fluid employed represents a function of the alkalinity of the waste's solid phase. Following extraction, the liquid extract was separated from the solid phase by filtration through a 0.45 μm glass fiber filter.^[36]

According to ISO 11885:2007 standard,^[37] concentrations of Sb, Ba, Cr, Mo, Ni, Se, As, Cd, Cs, Pb, Hg, V, and Ag were determined by induction coupled plasma mass spectrometry (ICP-MS, Agilent 7700), while the concentrations of Zn and Cu were determined by induction coupled plasma atomic emission spectrometry (ICP-AES, Ciros Vision Spectro). The content of chloride, fluoride, and sulfate ions was determined by the photometric method on a Hach Photometer DR3900. Leaching tests were done in duplicate.

The results were compared with limits given in the Annex 10 of the Regulation on categories, testing, and classification of waste.^[35]

Table 1. CSFT grain size composition.

Grain size class, <i>d</i> [μm]	Mass, <i>m</i> [%]	Cumulative, <i>D</i> [%]
500–250	1.7	100.0
250–125	6.9	98.3
125–63	27.7	91.4
63–20	46.5	63.7
20–10	11.9	17.0
10–5	3.6	5.3
5–0	1.7	1.7

2.3. Sorption Screening Method

The sorption screening of inactive isotopes of Mn(II), Co(II), Ni(II), Zn(II), Cd(II), and Pb(II) ions onto CSFT was investigated due to the user friendliness of the experiments. Within the brief screening method, sorbed amounts (mmol g^{-1}) of only three initial concentrations of each ion, 2×10^{-4} , 5×10^{-4} , and $1 \times 10^{-3} \text{ mol L}^{-1}$, were determined. The solutions were prepared using nitrate salts of the investigated cations (Merck, p.a.). Initial pH values of the solutions were in the range of 5.0–5.9, and they were applied without any adjustments. The amount of 0.1 g CSFT was shaken with 20 mL of appropriate cation solution on a rotary shaker at 10 rpm, at ambient temperature. Based on previous experiments, the contact time for equilibration was set at 48 h, suspensions were centrifuged (at 9000 rpm for 10 min), and filtered.^[11–12,14] Initial and concentration after sorption were measured by atomic absorption spectrometry (AAS, Perkin Elmer 3100).^[11–12,14] AAS was calibrated using standard solutions prepared by dilution of single element standards (1000 mg L^{-1} , Perkin Elmer). During the measurements, the calibration was checked at regular intervals. Sorption experiments were performed in triplicate, and results are presented as the mean values with corresponding absolute errors.

3. Results and Discussion

3.1. CSFT Characterization

3.1.1. Grain Size Analysis

The grain size composition of CSFT is shown in **Table 1**.

The grain size analysis showed that CSFT represents a fine-grained material. Fine particles, $<20 \mu\text{m}$, account for 17%. However, the particles with a diameter <250 and $63 \mu\text{m}$ account for approximately 98 and 63%, respectively.

These results were expected since flotation represents a process requiring fine granulation material, especially copper slag flotation, in which requirements regarding grain size composition are even stricter. It can be concluded that the grain size composition of CFST can have a positive effect on the sorption process because the finer the grain size is, the larger its specific surface area is, and thus the sorption process could be more efficient.^[38]

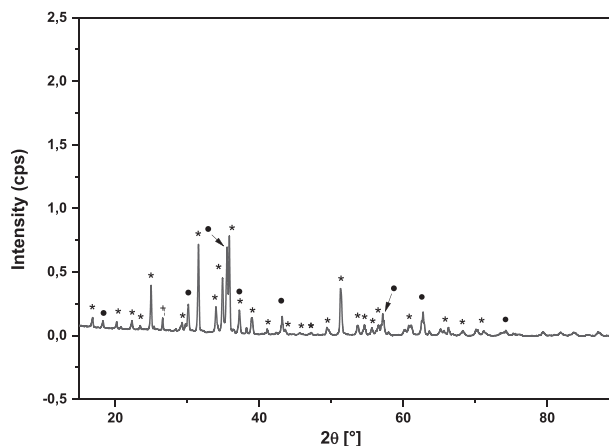


Figure 1. XRD pattern of CSFT sample. Symbols: magnetite (●), fayalite (*), and quartz (+).

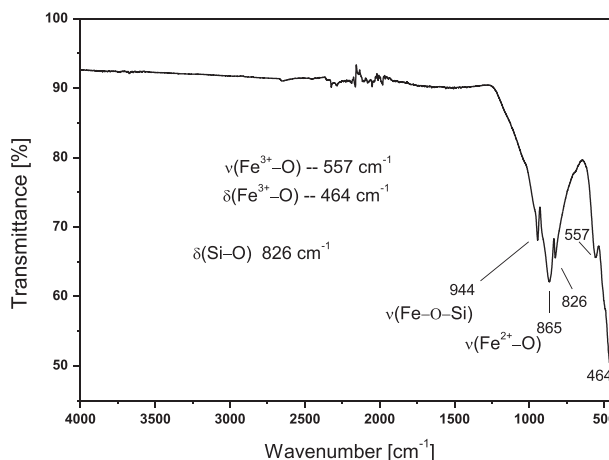


Figure 2. FT-IR spectrums of CSFT.

3.1.2. Mineral Composition (XRD analysis)

XRD analysis detected magnetite (Fe_3O_4) and fayalite ($\text{Fe}_2(\text{SiO}_4)$) as the most abundant minerals in CSFT (**Figure 1**).

Typical copper sulfide ores often contain various levels of iron sulfides and oxides. Magnetite is common in many ore deposits and host rocks, and its presence in CSFT was expected.^[39] Fayalite represents a ferrous iron silicate that belongs to the olivine minerals group. In CSFT, fayalite is the artificial mineral that arises in a high temperature process with low oxygen amount (calcination process) with a naturally elevated amount of silicon dioxide.^[40–41] Fayalite is the reaction product of magnetite and quartz under a reducing environment with low water content.^[42] It also was reported that the main constituents of copper smelter slags are FeO and SiO_2 , which are components of fayalite, with a share of 20–55 wt% worldwide.^[43] The high content of fayalite mineral phases in the investigated CSFT was expected based on its forming from the secondary smelting process of copper containing resources. The nature of this process is similar to crystallization in native silicate melts, i.e., volcanic lava or magma.^[44–45] Hence, the XRD peak position at approximately 2θ angle 26° most likely belongs to traces of pure quartz.^[46–47]

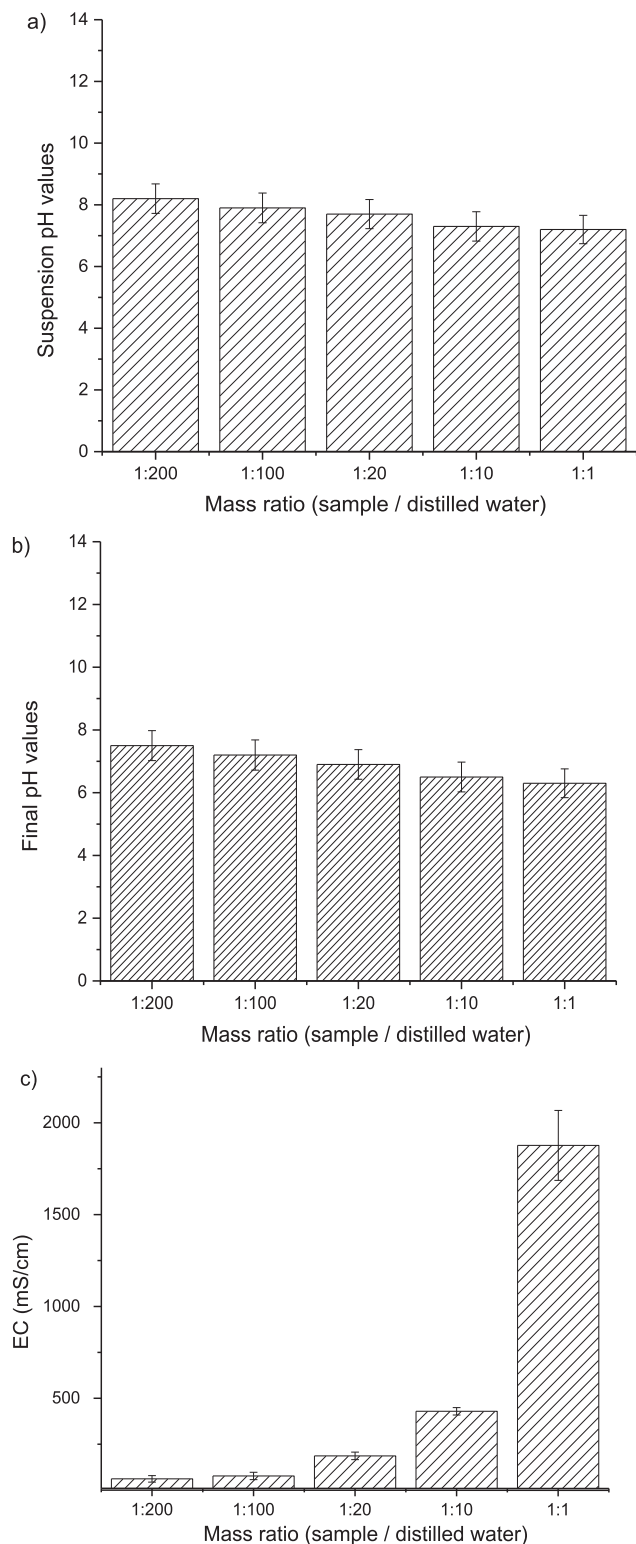


Figure 3. Relationships between solid/liquid ratios of CSFT: a) suspension pH values, b) filtrates final pH values, and c) EC of filtrates.

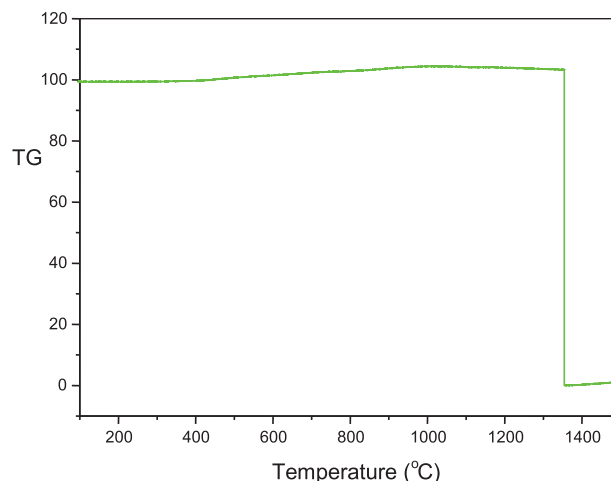


Figure 4. TGA plot.

3.1.3. FT-IR Analysis

The FT-IR spectrograms of CSFT (Figure 2) show the presence of Fe–O–Si group at 944 cm^{-1} , and Fe(II)–O at 865 and 826 cm^{-1} , as well as band characteristic for Si–O at 826 cm^{-1} . At wave numbers 557 and 464 cm^{-1} characteristic absorbance bands of Fe(III)–O groups are seen. The obtained FT-IR analysis results adequately match the composition detected by XRD.

3.1.4. Determination of pH and EC

Different quantities of CSFT were mixed with deionized water to achieve solid/solution ratios from 1:1 to 1:200. The pH values were measured in the suspension (Figure 3a) and then in the filtrates as a final pH (Figure 3b). Furthermore, after solid/liquid separation, the EC values of the filtrates were measured (Figure 3c). The results are shown with the corresponding standard deviation.

Along with the increase of solid/solution ratio, a slight drop in pH was observed. Measured electrical conductivity values increased with solid content increment. The increase was slight in solid/liquid ratio range from 1:200 to 1:10, whereas the increase was substantial for the 1:1 ratio. The EC increment was expected with elevated solid content due to a higher amount of dissolved minerals.

3.1.5. TGA and Determination of Characteristic Temperatures in Sample Melting Process

TGA results are shown as a TG curve, i.e., the mass loss (%) as a function of temperature (Figure 4).

The results in the air stream showed that at temperatures $<100\text{ °C}$ there was no change in the test sample mass, i.e., there was absence of free moisture. No changes in the sample mass were detected in the temperature range of $100\text{--}110\text{ °C}$, indicating absence of capillary water. Likewise, no changes in mass at temperatures from 550 to 1300 °C suggest that the sample does not contain any carbonates, sulfates, and sulfides since their decomposition occurred at temperatures $<1300\text{ °C}$.^[48–49] The expected

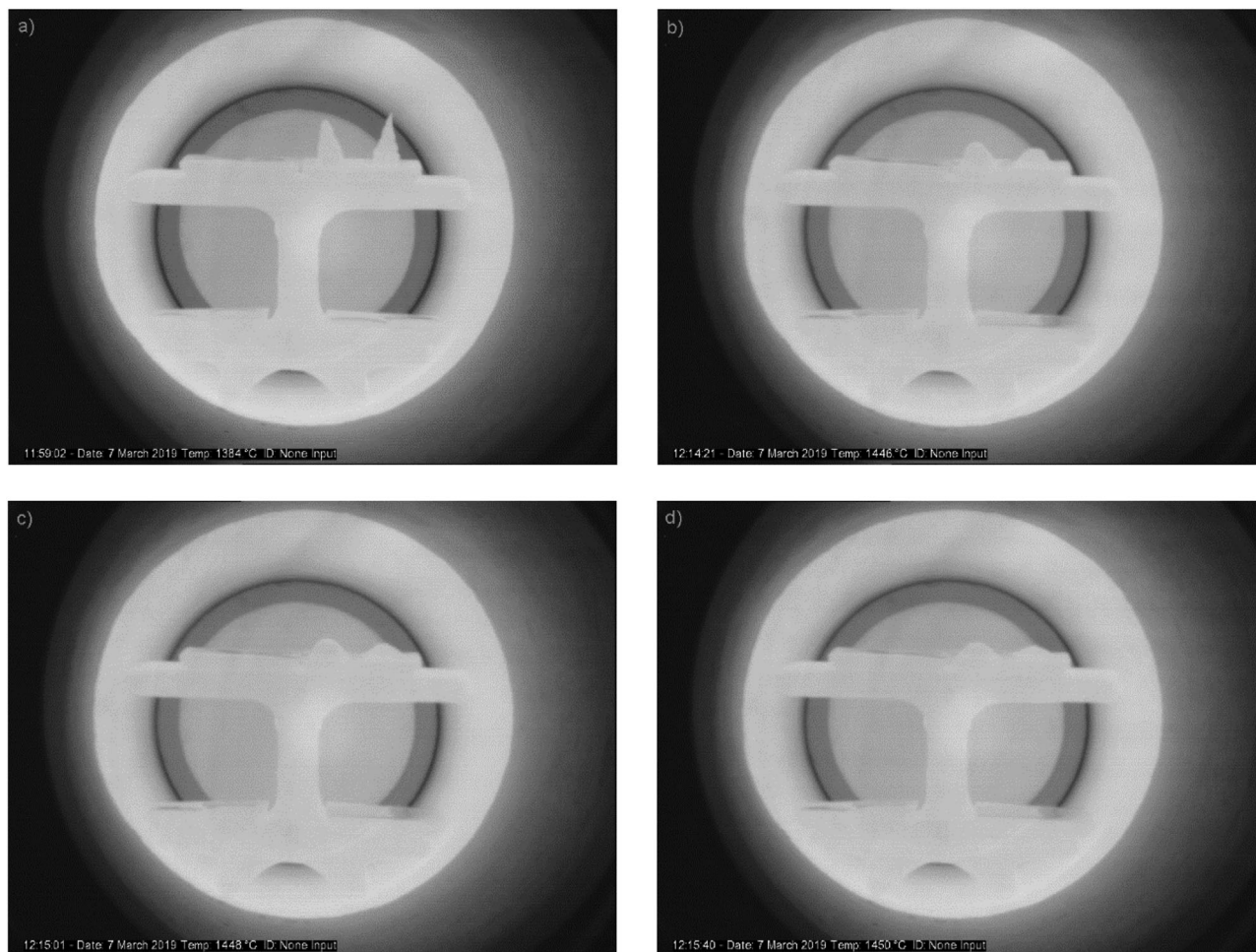


Figure 5. Melting process sample change: a) deformation temperature, b) sphere temperature, c) hemisphere temperature, and d) flow temperature.

lowest melting point was about 1270 °C, based on XRD analysis which detected fayalite and magnetite as the most abundant minerals in CSFT.^[50–51]

During the TGA investigation, exposure to a temperature higher than approximately 1300 °C induced a mass decrease of the studied sample, indicating its melting. Confirmation was given by determination of four characteristic temperatures in the melting process: deformation temperature, sphere temperature, hemisphere temperature, and flow temperature in the furnace for fusibility (**Figure 5**). The sample melting process started at 1384 °C, which was consistent with TGA results and XRD analysis.

3.2. Leachability and Toxicity of CSFT

The results of LP test, implying the impact of CSFT on the environment, are shown in **Table 2**.

Since the reference pH value of the waste class without allocated danger category (H15), according to the Annex 7 of the Regulation on categories, testing, and classification of waste,^[35] is 6–13, the measured pH value was within the allowed limits. Likewise, the obtained results were strongly correlated with the

Table 2. LP results of CSFT.

Parameter	Measured value	Expanded uncertainty [%]
Temperature of eluate [°C]	19	±2.5
pH	6.34	±0.5
EC [$\mu\text{S cm}^{-1}$]	480	±0.15

result of a solid/liquid ratio, 1:10, achieved by the modified US EPA 9045D method.^[33] The EC value was below the maximum allowed value for surface water quality, class I by the Serbian legislature.^[52]

Tables 3 and **4** show the classification and toxicity of CSFT by LP and TCLP methods, respectively.

The results of the LP test of CSFT were under the legislation of inert waste type, except the concentration of sulfates which corresponds with the prescription of nonhazardous waste. The TCLP test results indicated that the test sample does not show toxicity characteristics. According to the obtained results, the CSFT satisfies all the requirements for application as a raw material in the industry.^[35]

Table 3. Classification of CSFT by LP method.

Parameter	Unit	Measured value	Expanded uncertainty [%]	Reference value for inert waste ^[35]	Reference value for nonhazardous waste ^[35]	Reference value for hazardous waste ^[35]
Sb	mg kg ⁻¹ ^a	<0.11	±13.40	0.06	0.7	5
Ba	mg kg ⁻¹	<0.09	±9.35	20	100	300
Cr	mg kg ⁻¹	<0.05	±12.41	0.5	10	70
Mo	mg kg ⁻¹	0.41	±13.30	0.5	10	30
Ni	mg kg ⁻¹	<0.07	±11.28	0.4	10	40
Se	mg kg ⁻¹	<0.33	±11.36	0.1	0.5	7
Zn	mg kg ⁻¹	<0.05	±10.49	4	50	200
Cu	mg kg ⁻¹	<0.05	±8.94	2	50	100
As	mg kg ⁻¹	<0.2	±10.19	0.5	2	25
Cd	mg kg ⁻¹	<0.08	±10.36	0.04	1	5
Pb	mg kg ⁻¹	<0.2	±9.49	0.5	10	50
Hg	mg kg ⁻¹	<0.005	±10.28	0.01	0.2	2
Cl ⁻	mg kg ⁻¹	16	±10.27	800	15 000	25 000
F ⁻	mg kg ⁻¹	<0.2	±10.2	10	150	500
SO ₄ ²⁻	mg kg ⁻¹	2200	±13.5	1000	20 000	50 000

^a Dried mass.

Table 4. Testing of toxic characteristics of CSFT by TCLP method.

Parameter	Unit	Measured value	Expanded uncertainty [%]	Reference value ^[35]
Sb	mg L ⁻¹	0.17	±13.40	15
Cr	mg L ⁻¹	0.016	±12.41	5
Mo	mg L ⁻¹	0.010	±13.30	350
Ni	mg L ⁻¹	0.030	±11.28	20
Se	mg L ⁻¹	<0.033	±11.36	1
Zn	mg L ⁻¹	0.40	±10.49	250
Cu	mg L ⁻¹	12.2	±8.94	25
As	mg L ⁻¹	0.16	±10.19	5
Cd	mg L ⁻¹	0.008	±10.36	1
Pb	mg L ⁻¹	0.89	±9.49	5
Hg	mg L ⁻¹	<0.0005	±10.28	0.2
V	mg L ⁻¹	<0.008	±10.28	24
Ag	mg L ⁻¹	<0.005	±10.27	5

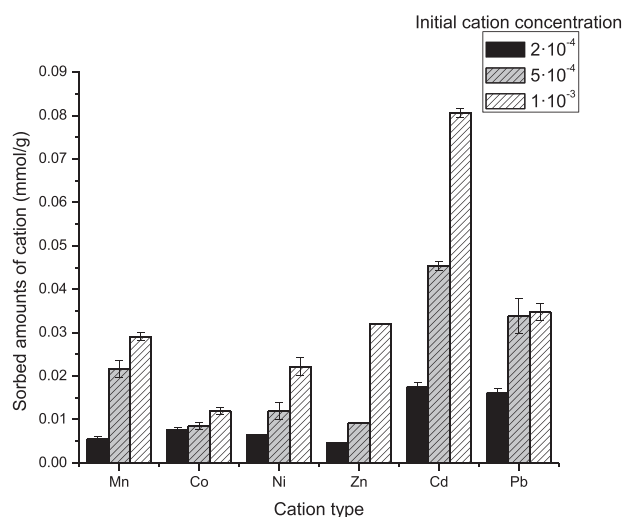


Figure 6. Sorbed quantities (Q_e) of investigated ions onto CSFT relative to each initial solution concentration.

3.3. Sorption Screening Method

The amounts of cations sorbed per unit mass of sorbent (Q_e) from a single-component solution are shown in relation to ion's initial concentrations with an appropriate standard deviation in **Figure 6**.

The sorption capacities decreased in the sequence Cd(II) > Pb(II) > Zn(II) > Mn(II) > Ni(II) > Co(II) for all initial cation concentrations. The sorption of Cd(II) ions at the concentration of 1×10^{-3} was the highest, with a sorption capacity of 0.08 mmol g⁻¹. Cd(II) showed the most efficient sorption for all initial concentrations, significantly higher than the other investigated ions. In the case of lower initial concentrations, the sorption capacities were far lower for all cations. The sorption of Pb(II), Zn(II), and Mn(II) were approximately twice lower than Cd(II) sorption at

the highest initial concentration with sorption capacities of 0.038, 0.032, and 0.029 mmol g⁻¹, respectively.

The obtained results were convenient to compare with sorption onto the main mineral constituents of CSFT, i.e., magnetite and fayalite, due to lack of CSFT sorption data. However, the sorption onto fayalite was not sufficiently investigated as well, except for arsenic ions sorption onto activated or calcinated minerals from the olivine group.^[28–29] Since these processes require energy, such modified sorbents cannot be considered cost-effective and environmentally friendly.

In the past decade, many studies indicated that magnetite nanoparticle composites could effectively remove a range of metal ions from water and wastewater solutions, e.g., copper, lead, cadmium, chromium, nickel, and zinc.^[30,53] Likewise,

Table 5. Sorption capacities of some investigated waste-based sorbents.

Waste-based sorbents	Sorption capacity [mmol g ⁻¹]						Reference
	Mn(II)	Co(II)	Ni(II)	Zn(II)	Cd(II)	Pb(II)	
Fly ash			0.007–0.017				[23]
Zeolite synthesized from fly ash		1.240	1.532	1.154		2.130	[24]
Raw red mud		0.520					[15]
Rinsed red mud			0.372				[16]
Treated animal bones		0.070–0.490					[17]
Treated sewage sludge			0.155				[18]
Blast furnace slag				0.350			[19]
					0.058	0.120	[20]
Seaweed biomass	0.160						[21]
Coal mine goafs	0.025				0.014	0.030	[22]
Concrete		0.270	0.130				[11]
Brick		0.050	<0.130				[11]
Hollow brick		0.030	0.170				[11]
Ceramic tiles		0.170	0.120				[12]
Roof tiles		0.065	0.100				[12]
Asphalt		0.060	<0.130				[11]
CSFT	0.029	0.012	0.022	0.032	0.081	0.035	This study

sorption of some radionuclides such as Cs(I), Eu(III), Co(II), Ni(II), Pb(II), Sr(II), and U(VI) by the magnetite-based composites could be very efficient.^[23,54] However, there is no sufficient data regarding the sorption of a wide range of radionuclides and heavy metals onto raw magnetite-based waste. Although magnetite-rich waste such as CSFT in this study showed inferior sorption results compared to artificial magnetite, it represents the low-cost and easily accessible sorbent against synthetic magnetite.

The sorption capacities of some waste-based sorbents are presented in **Table 5**.

Some of these materials exhibited higher sorption potential than CSFT, depending on the applied cation. However, sorption capacity is strongly associated with a number of experimental parameters such as pH value, contact time, sorbent particle size, i.e., sorbent specific surface area, solid/liquid ratio, and pretreatment (mechanical, thermal, and chemical modification). Consequently, the literature data cannot be directly compared.

4. Concluding Remarks

A preliminary investigation was performed concerning possible utilization of end waste from copper mining, i.e., CSFT in liquid radioactive waste treatment. CSFT contained fayalite and magnetite as the main mineral phases. According to pH, EC, TGA, characteristic temperatures in sample melting process, leachability, and toxicity tests, the investigated waste material satisfies all the requirements for application as a raw material. Sorption screening method showed that sorption capacities decreased in the sequence Cd(II) > Pb(II) > Zn(II) > Mn(II) > Ni(II) > Co(II) for all initial cation concentrations. At the highest investigated concentration level, the sorption of Cd(II) ions indicated a substantial immobilization potential with a sorption capacity of

0.08 mmol g⁻¹. The obtained results were compared with sorption onto magnetite and fayalite-based sorbents and literature data for other investigated waste-based sorbents. Despite better sorption onto magnetite and fayalite synthetic sorbents, CSFT showed satisfying potential as a low-cost and easily accessible sorbent. Compared to other waste-based materials, CSFT exhibited considerable potential, although it claims further investigation and optimization of experimental conditions to acquire higher sorption capacities.

Acknowledgements

The research presented in this paper was conducted with financial support of the Ministry of Education, Science and Technological Development of the Republic of Serbia, within the funding of scientific research work at the University of Belgrade, Vinca Institute of Nuclear Sciences (Contract No. 451-03-9/2021-14/200017); the University of Belgrade, Technical Faculty in Bor (Contract No. 451-03-9/2021-14/200131); Institute of Mining and Metallurgy (Contract No. 451-03-9/2021-14/200052); and the University of Belgrade, Faculty of Civil Engineering (No. 200092).

Conflict of Interest

The authors declare no conflict of interest.

Author Contributions

S.D. assisted in conceptualization, investigation, methodology, supervision, validation, writing original draft, and writing review and editing. I.J. assisted in conceptualization, formal analysis, investigation, resources, supervision, validation, writing original draft, and writing review and editing. M.S.-I. assisted in conceptualization, formal analysis, investigation, methodology, supervision, writing original draft, and writing review and

editing. Z.S. assisted in resources, writing original draft, and writing review and editing. V.G. assisted in formal analysis, investigation, and supervision. R.M. assisted in formal analysis and supervision. A.S. assisted in formal analysis, investigation, methodology, supervision, and writing review and editing.

Data Availability Statement

The data that support the findings of this study are available from the corresponding author upon reasonable request.

Keywords

flotation, recycling, reuse, slag, sorption

Received: January 19, 2021

Revised: August 28, 2021

Published online:

- [1] F. Carranza, N. Iglesias, A. Mazuelos, R. Romero, O. Forcat, *Miner. Eng.* **2009**, *22*, 107.
- [2] N. Karimi, R. Vaghar, M. R. Tavakoli Mohammadi, S. A. Hashemi, *J. Inst. Eng. India Ser. D* **2013**, *94*, 43.
- [3] Z. M. Stirbanovic, Z. S. Markovic, *Sep. Sci. Technol.* **2011**, *46*, 2496.
- [4] K. Murari, R. Siddique, K. K. Jain, *J. Mater. Cycles Waste Manage.* **2015**, *17*, 13.
- [5] B. Gorai, R. K. Jana, Premchand, *Resour. Conserv. Recycl.* **2002**, *39*, 299.
- [6] S. Pietrzyk, B. Tora, *Mater. Sci. Eng.* **2018**, *427*, 012002.
- [7] B. Golomeov, M. Golomeov, B. Krstev, A. Krstev, *Prospect. Innov. Econ. Bus.* **2011**, *7*, 80.
- [8] D. Panias, *Metallurgy* **2006**, *12*, 239.
- [9] E. Alonso, A. Gens, *Geotechnique* **2006**, *56*, 165.
- [10] T. S. Gabasiane, S. Bhero, G. Danha, *Procedia Manuf.* **2019**, *35*, 494.
- [11] I. Jelic, M. Sljivic-Ivanovic, S. Dimovic, D. Antonijevic, M. Jovic, M. Mirkovic, I. Smiciklas, *J. Cleaner Prod.* **2017**, *171*, 322.
- [12] I. Jelic, M. Sljivic-Ivanovic, S. Dimovic, D. Antonijevic, M. Jovic, R. Serovic, I. Smiciklas, *Process Saf. Environ. Prot.* **2016**, *105*, 348.
- [13] M. Sljivic-Ivanovic, I. Jelic, A. Loncar, D. Nikezic, S. Dimovic, B. Loncar, *Nucl. Technol. Radiat. Prot.* **2017**, *32*, 281.
- [14] M. Sljivic-Ivanovic, I. Jelic, S. Dimovic, D. Antonijevic, M. Jovic, A. Mrakovic, I. Smiciklas, *Clean Technol. Environ.* **2018**, *20*, 1343.
- [15] A. Milenković, I. Smičiklas, J. Marković, N. Vukelić, *Nucl. Technol. Radiat.* **2014**, *29*, 79.
- [16] S. Smiljanić, I. Smičiklas, A. Perić-Grujić, B. Lončar, M. Mitrić, *Chem. Eng. J.* **2010**, *162*, 75.
- [17] S. Dimović, I. Smičiklas, I. Plečaš, D. Antonović, M. Mitrić, *J. Hazard. Mater.* **2009**, *164*, 279.
- [18] Y. Zhai, X. Wei, G. Zeng, D. Zhang, K. Chu, *J. Sep. Purif. Technol.* **2004**, *38*, 191.
- [19] L. Blahova, M. Mucha, Z. Navratilova, S. Gorošova, *Inz. Miner.* **2015**, *36*, 89.
- [20] X. Chen, W. Hou, Q. Wang, *Huan Jing Ke Xue* **2009**, *30*, 2940.
- [21] N. L. Nafie, D. P. Ayunita, P. Taba, *Earth Environ. Sci.* **2020**, *473*, 012075.
- [22] Q. Yao, Z. Xia, C. Tang, L. Zhu, W. Wang, T. Chen, Y. M. Tan, *Geofluids* **2020**, *1*, 8560151.
- [23] B. Bayat, *J. Hazard. Mater.* **2002**, *95*, 251.
- [24] W. Qiu, Y. Zheng, *Chem. Eng. J.* **2009**, *145*, 483.
- [25] International Atomic Energy Agency, *Technical Reports*, Series No. 389, Vienna, Austria **1998**.
- [26] J. I. R. Silva, A. C. M. Ferreira, A. C. A. Costa, *J. Radioanal. Nucl. Chem.* **2009**, *279*, 909.
- [27] W. T. Chen, M. F. Zhou, X. Li, J. F. Gao, K. Hou, *Ore Geol. Rev.* **2015**, *65*, 929.
- [28] Z. Bujňáková, E. Turianicová, P. Baláž, *Acta Montan. Slovaca* **2012**, *2*, 137.
- [29] L. Carlos, F. S. G. Einschlag, M. C. González, D. O. Mártire, in *Waste Water*, Vol. 2013 (Eds: F. S. G. Einschlag), IntechOpen, London **2013**, Ch. 3.
- [30] M. R. Lasheena, I. Y. El-Sherif, D. Y. Sabry, S. T. El-Wakeela, M. F. El-Shahat, *Desalin. Water Treat.* **2016**, *57*, 17421.
- [31] ISO 17892-4:2016, *International Organization for Standardization*, Geneva, Switzerland **2016**.
- [32] International Centre for Diffraction Data, ICDD, *Powder Diffraction File—Announcement of New Database*, International Centre for Diffraction Data, PA **2012**.
- [33] Environmental Protection Agency SAD, US EPA, *Reference Methodology: Method 9045D, Soil and Waste pH*, Washington, DC **2002**.
- [34] SRPS EN 12457-2:2008, Characterization of waste—Leaching—Compliance test for leaching of granular waste materials and sludges—Part 2: One stage batch test at a liquid-solid ratio of 10 l/kg for materials with a high content solids and particle size of less than 4 mm (with decreasing particle size, or without decreasing), Institute for Standardization of Serbia, Belgrade, Serbia **2008**.
- [35] R. S. Off. Gazette, Regulation on categories, testing, and classification of waste, Official Gazette of the Republic of Serbia, No. 56/2010 **2010**.
- [36] Environmental Protection Agency USA, US EPA, *Method 1311: Toxicity Characteristic Leaching Procedure*, Environmental Protection Agency, Washington, DC **1992**.
- [37] ISO 11885:2007, *Water quality—Determination of selected elements by inductively coupled plasma optical emission spectrometry (ICP-OES)*, International Organization for Standardization, Geneva, Switzerland **2007**.
- [38] K. Unger, F. Vydra, *J. Inorg. Nucl. Chem* **1968**, *30*, 1075.
- [39] B. Li, Y. Wei, H. Wang, Y. Yang, *ISIJ Int.* **2018**, *58*, 1168.
- [40] V. Sibanda, E. Sipunga, G. Danha, T. A. Mamvura, *Heliyon* **2020**, *6*, 03135.
- [41] A. Mucke, *J. Afr. Earth Sci.* **2003**, *36*, 55.
- [42] X. Wang, D. Geysen, T. Padilla, H. D. D'Hoker, S. Huang, P. T. Jones, T. Van Gerven, B. Blanpain, presented at The Second International Slag Valorization Symposium, Leuven, Belgium, April **2011**.
- [43] I. Michailova, D. Mehandjiev, *J. Chem. Technol. Metall.* **2010**, *45*, 317.
- [44] H. Shi, L. Chen, A. Malfliet, T. P. Jones, B. Blanpain, M. Guo, presented at The 10th International Conference on Molten Slags, Fluxes and Salts, Seattle, WA, May **2016**.
- [45] J. Chisholm, *Ann. Occup. Hyg.* **2005**, *49*, 351.
- [46] A. Lin, *Fossil Earthquakes: The Formation and Preservation of Pseudotachylites*, Springer, Berlin **2007**.
- [47] J. L. Mier Buenhombre, in *Thermal Analysis, Fundamentals and Applications to Material Characterization* (Ed: R. A. Diaz), Escuela Politécnica Superior da Coruna, Mendizabal, Spain **2005**, p. 99.
- [48] S. Prasad, B. D. Pandey, *J. Therm. Anal. Calorim.* **1999**, *58*, 625.
- [49] F. C. Kracek, *Melting and Transformation Temperatures of Mineral and Allied Substances*, Government Printing Office, Washington, DC **1963**.
- [50] S. J. Schneider, *Compilation of the Melting Points of the Metal Oxides, Monograph, 68 Issued*, National Bureau Of Standards, United States Department of Commerce, Gaithersburg, MD **1963**.
- [51] RS Off. Gazette, Regulation on limit values of pollutants in surface and groundwater and sediment and deadlines for their achievement. Official Gazette of the Republic of Serbia, No. 50/2012 **2012**.
- [52] S. A. Baig, T. T. Sheng, C. Sun, X. Q. Xue, L. S. Tan, X. H. Xu, *PLoS One* **2014**, *9*, e100704.
- [53] A. Egorin, E. Tokar, A. Kalashnikova, T. Sokolnitskaya, I. Tkachenko, A. Matskevich, E. Filatov, L. Zemskova, *Materials* **2020**, *13*, 1189.
- [54] M. Syed, S. M. Husnain, W. Um, C. Woojin-Leed, Y. S. Chang, *RSC Adv.* **2018**, *8*, 2521.